NJC

New Journal of Chemistry

An international journal of the chemical sciences

www.rsc.org/njc

Volume 33 | Number 12 | December 2009 | Pages 2357–2496

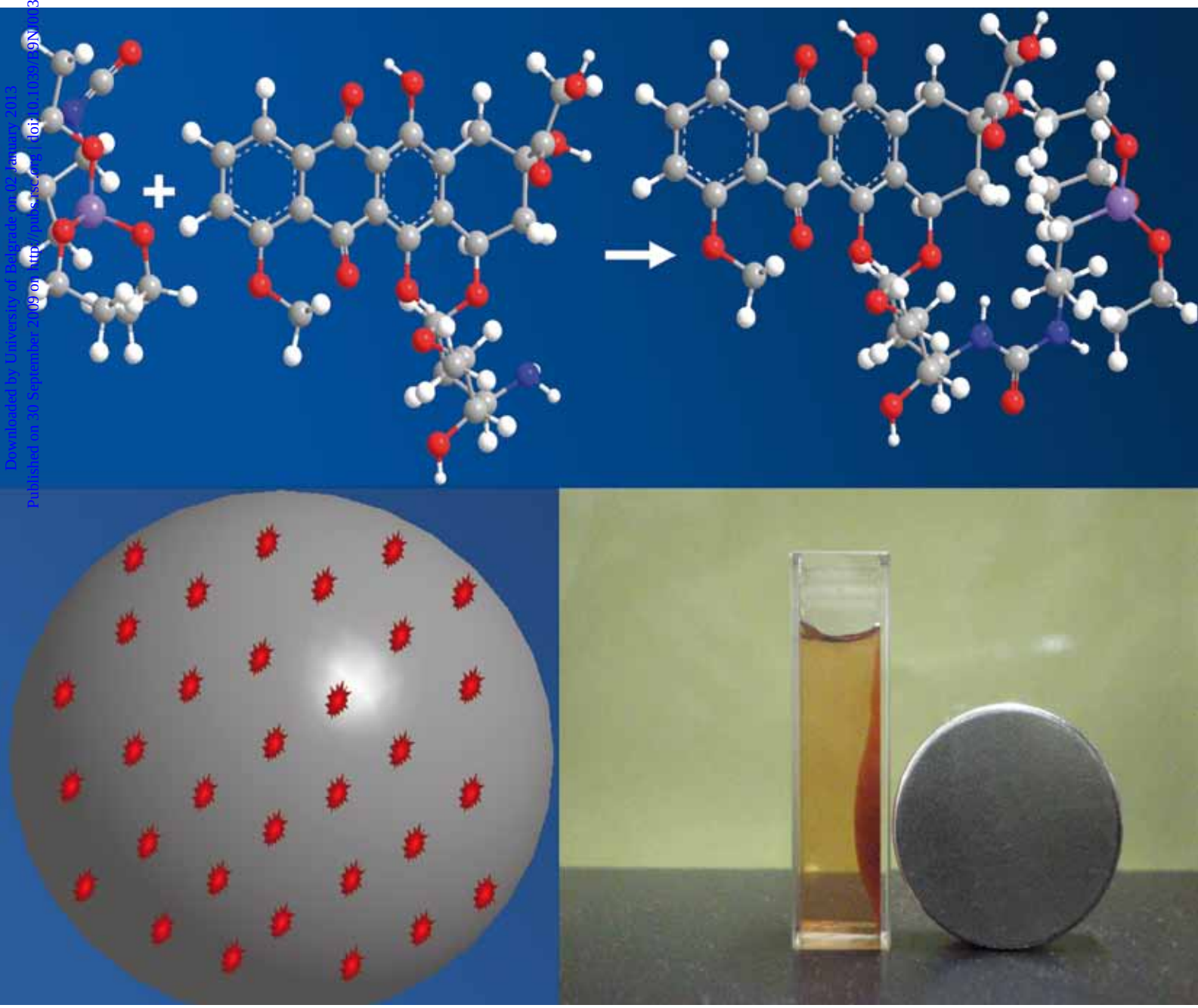

ISSN 1144-0546

RSC Publishing

PAPER

Zhifei Dai *et al.*

One-pot construction of doxorubicin conjugated magnetic silica nanoparticles

One-pot construction of doxorubicin conjugated magnetic silica nanoparticles†

Shouzhu Li, Yan Ma, Xiuli Yue,* Zhong Cao and Zhifei Dai*

Received (in Montpellier, France) 18th July 2009, Accepted 24th August 2009
First published as an Advance Article on the web 30th September 2009
DOI: 10.1039/b9nj00342h

Doxorubicin (DOX) conjugated magnetic silica nanoparticles (DOX–Fe_3O_4–SiO_2) are successfully fabricated using a new one-pot method without need for the process of inconvenient multistep synthesis in advance, based on the condensation of DOX and the silica precursor 3-isocyanatopropyltriethoxysilane (ICPTES), followed by the spontaneous formation of a silica coating onto the surface of Fe_3O_4 nanoparticles *via* sol–gel polymerization of triethoxysilane. Mass spectroscopy provides evidence that doxorubicin is conjugated to ICPTES *via* a urea bond (–NHCONH–) *via* the reaction of the amino groups of DOX with the isocyanate group (–N═C═O) of ICPTES in water. The obtained magnetic nanoparticles are well dispersed. Their mean diameter is about 66.9 nm with a narrow size distribution. The conjugated DOX–SiO_2–Fe_3O_4 nanoparticles exhibited a higher loading efficiency of 60.5 ± 3.7% and a more sustained release profile than SiO_2 nanoparticles containing physically-entrapped DOX. It is anticipated that fine-tuning of other drugs or bioactive molecules containing –NH_2 groups to Fe_3O_4/SiO_2 nanoparticles would foster innovative avenues for the development of smart drug delivery and controlled release systems.

Introduction

Nowadays, the use of nanoparticles as therapeutic and diagnostic agents[1,2] is of intense interest owing to their unique properties such as large specific capacity for drug loading,[3–5] strong superparamagnetism,[6] efficient photoluminescence,[7,8] among others.[9–11] Fe_3O_4 magnetic nanoparticles, whose motion can be manipulated and controlled by an external magnetic field, have been sophisticatedly employed in many advanced technology areas including biology, pharmaceuticals and diagnostics.[12–14] A magnetically targeted drug-delivery system, involves binding a drug to small biocompatible magnetic particles, injecting these into the bloodstream and using a high gradient magnetic field to pull them out of suspension in the target region. Once located on the vessel wall the drug can either be released directly into the blood stream or a biological technique can be used to ensure uptake of the particles into the tissue, which may lead to a tissue-specific delivery of drugs, and so avoiding side effects.[15]

To deliver drugs to specific organs, a great variety of organic systems, such as liposomes and polymeric nanoparticles, have been developed. However, they suffer from limitations, including poor stability, and rapid elimination by the immune system. On the contrary, silica particles are stable, non-toxic and highly biocompatible, offering a viable alternative.[16] In addition, silica-coated magnetic nanocomposites show great a stability against coagulation and full protection of iron oxide substrate particles from leaching in an acidic environment. Bioactive molecules can be easily encapsulated within silica particles. Silica particles have surfaces decorated with hydroxyl groups that render them intrinsically hydrophilic, which can decrease oxide particle clearance by the reticuloendothelial system (RES), and thus increase their circulation time in the blood. As the drug carrier material, silica is not subjected to microbial attack and it neither swells nor changes porosity in response to the environmental pH.[17]

DOX has been extensively used for the treatment of several forms of cancers, but its cytotoxicity to normal tissue and inherent multidrug resistance effect remain as major problems to be solved.[18–27] In some studies, DOX has been covalently linked to polymer carriers through a route of complicated organic synthesis.[28–30] Recently DOX was successfully grafted to Fe_3O_4@SiO_2 core–shell structure nanoparticles *via* an amide bond by a multistep process.[31] In this study, a novel one-pot method was developed for the preparation of DOX bonded magnetic silica nanoparticles (DOX–Fe_3O_4–SiO_2) based on the condensation of DOX and silica precursor of 3-isocyanatopropyltriethoxysilane (ICPTES) through a urea bond (–NHCONH–),[32] followed by the spontaneous formation of a silica shell onto the surface of Fe_3O_4 nanoparticles *via* sol–gel polymerization of triethoxysilane (Scheme 1). It is advantageous to have no need for the process of inconvenient organic synthesis in advance. The morphology and chemical components of the obtained DOX–Fe_3O_4–SiO_2 nanoparticles were characterized by mass spectrometry (MS) transmission electron microscopy (TEM), Fourier transform infrared spectroscopy (FT-IR), X-ray photoelectron spectroscopy (XPS) and powder X-ray diffraction (XRD). The release

Nanobiotechnology Division, State Key Laboratory of Urban Water Resources and Environment, School of Sciences, Harbin Institute of Technology, Harbin 150001, China. E-mail: zhifei.dai@hit.edu.cn, xiulidx@yahoo.com.cn; Fax: +86 451 86402692; Tel: +86 451 86402692

† Electronic supplementary information (ESI) available: Fig. S1: DLS size distribution profiles. Fig. S2: Mass spectra of the mixture of DOX and ICPTES after sonication. See DOI: 10.1039/b9nj00342h

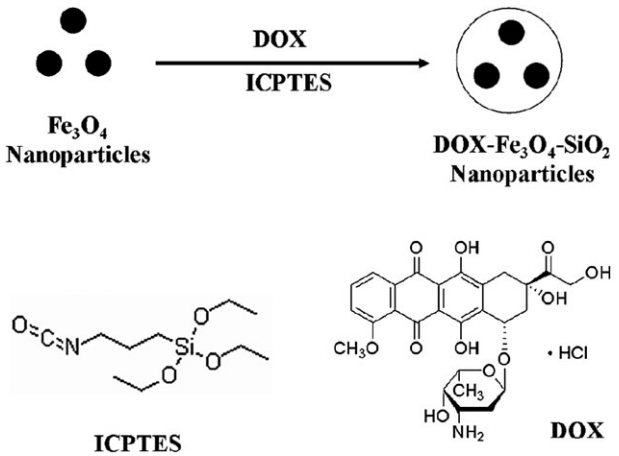

Scheme 1 Schematic representation of the preparation process of doxorubincin conjugated Fe_3O_4–SiO_2 nanoparticles.

property of the DOX loaded nanoparticles was also studied *in vitro*.

Experimental

Materials

3-Isocyanatopropyltriethoxysilane (ICPTES, 99%) was obtained from Diamond Advanced of Chemical Inc. Doxorubicin hydrochloride (DOX·HCl) was purchased from Beijing Huafeng United Technology. Tetraethyl orthosilicate (TEOS 99.9%) was obtained from Aldrich. Other chemicals were purchased from Beijing Chemical Company. All chemicals are of analytical grade and used directly without further purification.

Synthesis of the citric acid modified Fe_3O_4 nanoparticles

Fe_3O_4 nanoparticles were synthesized by a co-precipitation method. An aqueous solution containing 2 mM $FeCl_3$ and 1 mM $FeSO_4$ in a 500 mL flask was heated to 70 °C under N_2. Then, 30 mL $NH_3{\cdot}H_2O$ was added dropwise under vigorous stirring for 2 h. To obtain the well-dispersed Fe_3O_4 nanoparticles, citric acid was added under 80 °C with another vigorous stirring for 2 h. The black precipitate was isolated by an Nd–Fe–B magnet and washed twice with deionized water and three times with ethanol. Then the collected magnetic nanoparticles were dispersed in water for use.

Synthesis of the DOX conjugated Fe_3O_4–SiO_2 nanoparticles

The freshly prepared Fe_3O_4 nanoparticles (0.040 mL, 8.43 mg mL^{-1}), doxorubincin hydrochloride (2.0 mg) and ICPTES (4.0 mg) were mixed in 10 mL deionized water. 1 mL of 0.2 M Na_2HPO_4 was added to catalyze the reaction system. Then, the solution was treated by ultrasonication for 10 min. The reaction was allowed to hydrolyze and polymerize at room temperature for 24 h to obtain the DOX conjugated Fe_3O_4–SiO_2 nanoparticles. SiO_2 containing physically-entrapped DOX was prepared according to the same procedure with TEOS.

Characterization

Fourier transform infrared (FT-IR) spectra were recorded (128 scans with a resolution of 4 cm^{-1}) on a Varian FTS 3100 Fourier transform infrared spectrophotometer. XRD patterns were recorded on Rigaku-D/2500V diffractometer using Cu-Kα radiation (λ = 1.5418 Å, 2θ = 10–70°). The mass spectra (MS) were directly obtained by injecting the aqueous solution of the mixture to an API 3000 LC/MS/MS System. TEM images were obtained using an H-7650 with a tungsten filament at an accelerating voltage of 200 kV. The particle size distributions were determined by a 90Plus/BI-MAS instrument (Brookhaven Instruments Co., USA). The surface element binding energy and chemical composition of the particles were characterized by a VGESCALAB MKII X-ray photoelectron spectrometer. Drug loading capacity and release behavior were determined using a Varian 4000 UV-vis spectrophotometer.

Analysis of DOX release from magnetic SiO_2 nanoparticles

DOX-conjugated Fe_3O_4–SiO_2 nanoparticles were suspended in 10 mL of phosphate buttered saline (PBS) solution at room temperature. The DOX released into the incubation medium was sampled at pre-determined time intervals after separating particles and the released DOX with an Nd–Fe–B magnet. The release amount was determined from the absorbance at 480 nm by UV/vis spectrophotometry. The drug loading content and encapsulation efficiency were obtained by eqn (1) and eqn (2), respectively.

$$\text{Drug loading content}\ (\%) = \frac{\text{Weight}_{\text{drug in particles}}}{\text{Weight}_{\text{particles}}} \times 100\% \quad (1)$$

$$\text{Encapsulation efficiency}\ (\%) = \frac{\text{Weight}_{\text{loaded drug}} - \text{Weight}_{\text{free drug}}}{\text{Weight}_{\text{loaded drug}}} \times 100\% \quad (2)$$

Results and discussion

Fabrication of Fe_3O_4 nanoparticles and DOX–SiO_2–Fe_3O_4 nanoparticles

The Fe_3O_4 nanoparticles were fabricated by co-precipitation of ferrous and ferric cations using $NH_3{\cdot}H_2O$ according to the widely applied method.[31] Citric acid was used to modify the magnetic particles, rendering the Fe_3O_4 nanoparticles well dispersed in water for the further silica coating.[33] The DLS size distribution profile of the citric-acid-modified magnetic nanoparticles is shown in Fig. 2(a). The modified magnetic nanoparticles are well dispersed. The average particle size is about 13.7 nm with a narrow size distribution. The maximum critical size for Fe_3O_4 nanoparticles in the superparamagnetic state is approximately 20 nm. Penetration of the nanoparticles into the extracellular matrix of solid tumors is limited to particles smaller than 100 nm.[34] Therefore, the synthesized particles with a mean size of about 13.7 nm are suitable for *in vivo* biological applications.[35]

The obtained Fe_3O_4 nanoparticles were then mixed with DOX·HCl and ICPTES by ultrasonication in aqueous solution. After the dissociation of hydrogen ions from $-NH_3^+$ groups with Na_2HPO_4, the DOX-siloxane intermediate compound could form through the reaction of the reactive groups of DOX with the isocyanate group (–N═C═O) of the alkoxysilane precursor, ICPTES. This reaction may produce either urea (–NHCONH–) or urethane (–NHCOO–) groups, which form bridges between the DOX and the inorganic matrix. The former linkage (–NHCONH–) should be preferentially formed as $-NH_2$ groups react much faster with isocyanates than –OH groups due to the high selectivity between the isocyanate group of ICPTES and the amino group of DOX in aqueous solution.[36] The formation of the intermediate of DOX and ICPTES was proved by mass spectra (Fig. 1, *m*/*z*: calc. for $C_{37}H_{50}N_2O_{15}Si$: 790.88; found: 791.7 $[M + H]^+$ and 813.6 $[M + Na]^+$). Then, sol–gel processes ($Si–OCH_3CH_2 + H_2O \rightarrow Si–OH + CH_3CH_2OH$ followed by $Si–OH + Si–OH \rightarrow Si–O–Si + H_2O$) occurred on the surface of Fe_3O_4 nanoparticles, resulting in the DOX–SiO_2–Fe_3O_4 nanoparticles. The silica-coated magnetic nanoparticles are well dispersed. The DLS measurement showed that the mean diameter of the coated particles is about 66.9 nm with a narrow size distribution (Fig. 2(b)). They are much bigger than the Fe_3O_4 nanoparticles (13.7 nm) due to the polymerization of the DOX conjugated silane on the surface of Fe_3O_4 nanoparticles.

Fig. 3(a) shows a TEM image of the prepared DOX–SiO_2–Fe_3O_4 nanoparticles. After drying, the DOX–SiO_2–Fe_3O_4 nanoparticles grouped in clusters, but individual DOX–SiO_2–Fe_3O_4 nanoparticles retained their perfectly spherical shape and integrity. It could be clearly seen that Fe_3O_4 existed as darker dots in the particles. Transmission electron micrographs showed DOX–SiO_2–Fe_3O_4 nanoparticles with a diameter of approximately 60 nm, almost in agreement with the hydrodynamic diameter (66.9 nm) evaluated by DLS measurements (Fig. 2(b)). Aggregate formation resulted from interactions occurring between the OH groups of the silanols when the individual particles were brought into contact.[37] The DOX–Fe_3O_4–SiO_2 nanoparticles showed a good response to a magnetic field (Fig. 3(b)), indicating that the magnetic DOX–Fe_3O_4–SiO_2 particles would have great potential application in the treatment of cancer using magnetic targeting drug-delivery technology.

XPS measurements were used to confirm the combination of magnetic particle cores and silica coating. The X-ray photoelectron spectra (XPS) of bare magnetic particles and

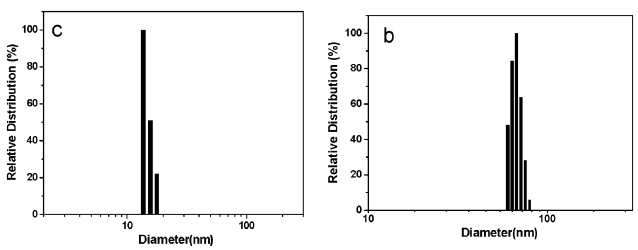

Fig. 1 DLS size distribution profiles: (a) the citric acid modified Fe_3O_4 nanoparticles, (b) the DOX–Fe_3O_4–SiO_2 nanoparticles.

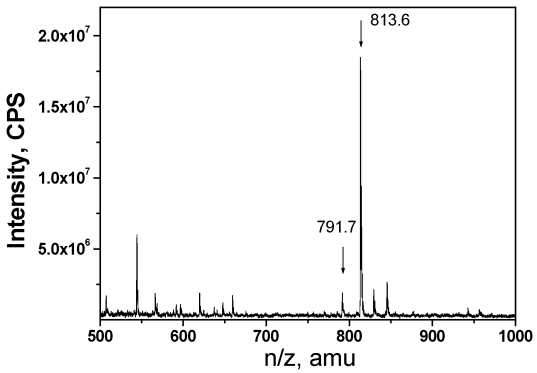

Fig. 2 Mass spectra of the mixture of DOX and ICPTES after sonication.

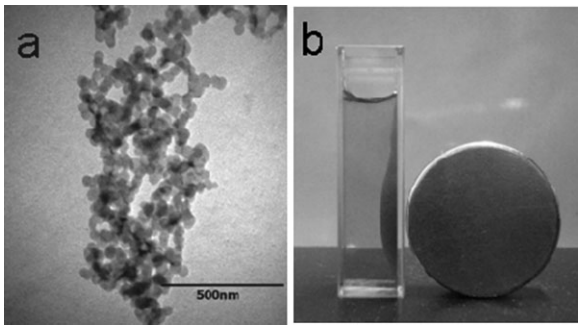

Fig. 3 (a) TEM image and (b) photograph under a magnetic field of DOX–Fe_3O_4–SiO_2 nanoparticles.

DOX–Fe_3O_4–SiO_2 structured materials are shown in Fig. 4. The Si 2p peak of the DOX–Fe_3O_4–SiO_2 sample is observed at 103.5 eV in Fig. 4(a), which arises from the silica coating. The O 1s binding energy for the bare magnetic nanoparticles was 530.5 eV, which was close to previously reported values,[38] but lower than that of the DOX–Fe_3O_4–SiO_2 particles by 2.1 eV (Fig. 4(b)). The latter exhibited a broad peak at 532.6 eV due to the formation of the Fe–O–Si chemical bond. The electronegativity of Si is higher than that of Fe, leading to the lower electronic density on the surface of the Fe. The formation of Fe–O–Si bonds on the surface of the DOX–Fe_3O_4–SiO_2 particles reduced the electronic density of O, resulting in a chemical shift of 2.1 eV. In agreement with the values reported in the literature,[38] the Fe $2p_{3/2}$ and Fe $2p_{1/2}$ binding energies of the bare magnetic nanoparticles were 711.4 and 724.8 eV, respectively. The corresponding signals were much weaker for DOX–Fe_3O_4–SiO_2 (Fig. 4(c)) providing evidence for the silica coating on the Fe_3O_4 magnetic nanoparticles by the sol–gel process.

Fig. 5 shows XRD patterns of the Fe_3O_4 nanoparticles and the DOX–Fe_3O_4–SiO_2 nanoparticles. A series of characteristic peaks in the spectrum of Fig. 5(a) at 2.968 (2 2 0), 2.535 (3 1 1), 2.103 (4 0 0), 1.719 (4 2 2), 1.614 (5 1 1), 1.478 (4 4 0) and 1.271 (5 3 3) matched well with the reported value (JCPDS no. 65–3107). The *d* values worked out from the XRD spectrum were well indexed to a pure cubic inverse spinel phase of Fe_3O_4. The same characteristic peaks can also be found in the spectrum of Fig. 5(b). The average particle size of Fe_3O_4 calculated from the reflection peak of (311) was about 13 nm

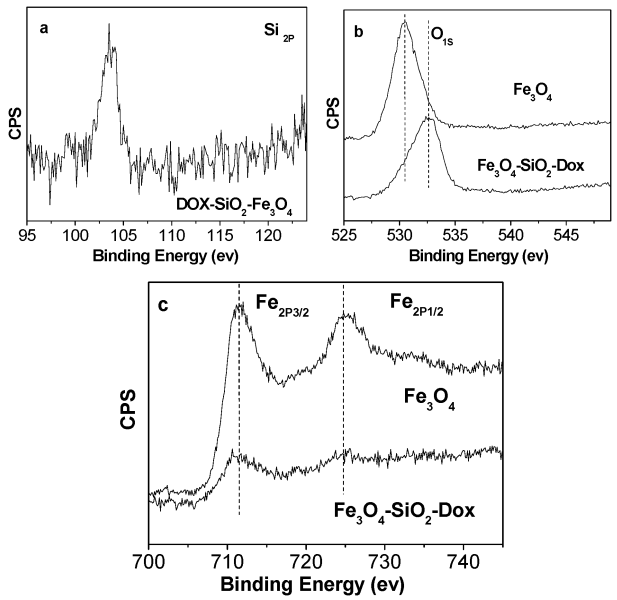

Fig. 4 XPS spectra of (a) Si 2p, (b) O 1s and (c) Fe 2p of prepared Fe_3O_4 and DOX–SiO_2–Fe_3O_4.

for DOX–Fe_3O_4–SiO_2 using the Scherrer equation: $D = K\lambda/\beta\cos\theta$, where K is the Scherrer constant, λ the X-ray wavelength, β the peak width of half-maximum, and θ is the Bragg diffraction angle. It suggested that the crystalline structure of Fe_3O_4 nanoparticles did not change after the surface modification with sodium citrate and silica. The presence of a broader hump at $2\theta = 22.5^\circ$ illustrated that the silica was amorphous. The intensities of the diffraction peaks corresponding to Fe_3O_4 in DOX–Fe_3O_4–SiO_2 nanoparticles were seen to decrease greatly due to the shielding effect of amorphous silica coating. Thus, the XRD results proved the formation of DOX–Fe_3O_4–SiO_2 conjugated nanoparticles.

FTIR spectroscopy was used to further confirm that DOX was successfully immobilized on the nanoparticles of Fe_3O_4–SiO_2. FTIR spectra of Fe_3O_4, free DOX and the DOX–Fe_3O_4–SiO_2 conjugated nanoparticles are shown in Fig. 6(a), (b) and (c), respectively. Free DOX showed a characteristic IR absorption band at 1734 cm^{-1} due to the stretching vibration of the carbonyl group at the 13-keto position, bands at 1614 and 1585 cm^{-1} due to the stretching

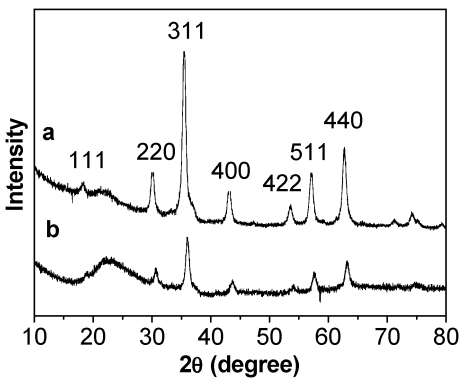

Fig. 5 XRD patterns of (a) Fe_3O_4 powder and (b) DOX–Fe_3O_4–SiO_2 powder.

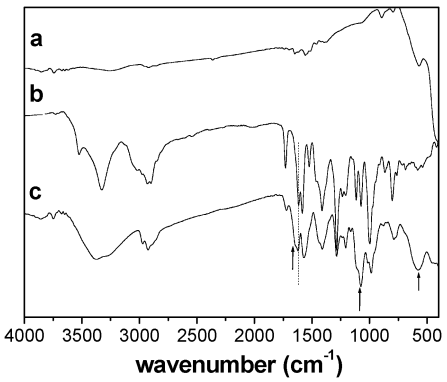

Fig. 6 FTIR spectra of (a) Fe_3O_4 nanoparticles, (b) free DOX and (c) DOX–Fe_3O_4–SiO_2 nanoparticles.

vibration of two carbonyl groups of the anthracene ring, a band at 1287 cm^{-1} due to the skeleton vibration of the DOX molecule, and a band at 998 cm^{-1} due to the stretching vibration of C–O bonds. In addition, the broad band near 3327 cm^{-1} refers to the vibration of the –OH groups with a contribution of $–NH_2$ within this band. After the formation of the DOX–Fe_3O_4–SiO_2 conjugated nanoparticles, a peak appeared at 578 cm^{-1} due to the characteristic vibration of Fe–O–Fe (Fig. 5(c)), indicating the presence of Fe_3O_4 magnetic nanoparticles. Compared the spectra of Fig. 6(b) and (c), a broad and strong band at 1074 cm^{-1} due to the stretching vibration of the characteristic Si–O–Si bond verified the formation of the silica. A shoulder peak appeared at 1650 cm^{-1} (above 1614 cm^{-1}) attributed to the characteristic C═O absorption from a urea link as shown in Fig. 5(c).[39] This demonstrates the successful silica coating and DOX conjugation on the surface of the magnetic nanoparticles in one step.

DOX release from DOX–Fe_3O_4–SiO_2 conjugated nanoparticles

The encapsulation efficiency of the DOX–SiO_2–Fe_3O_4 nanoparticles was evaluated to be 60.5 ± 3.7% and the drug loading content was about 39.4 ± 2.4%. In contrast, the control silica nanoparticles exhibited much lower loading efficiency (7.3 ± 1.6%) and drug loading content (12.7 ± 2.8%) The release profiles of DOX from DOX–Fe_3O_4–SiO_2 nanoparticles and the control silica nanoparticles are shown in Fig. 7. A "burst" release was observed for the control silica nanoparticles because DOX was only entrapped into silica nanoparticles physically. 90 ± 3.6% DOX was released from the silica nanoparticles within 22.5 h. Obviously, the conjugation of DOX molecules to the Fe_3O_4–SiO_2 nanoparticles resulted in significantly lower release rate. Over 261 h, only 13.3 ± 3.4% of the loaded drug was released from the DOX–Fe_3O_4–SiO_2 nanoparticles. The slower release rate for DOX–Fe_3O_4–SiO_2 nanoparticles was attributed to the urea linkage (–NHCONH–) between the DOX and the inorganic nanoparticles. The gradual hydrolysis of the weak urea bond in PBS leads to the slow release of DOX from the DOX–SiO_2–Fe_3O_4 nanoparticles. Since the urea linkage between DOX and SiO_2 could be hydrolyzed, the release of DOX might be accelerated under conditions of low pH around tumours and lysozymes inside the tumor cells.

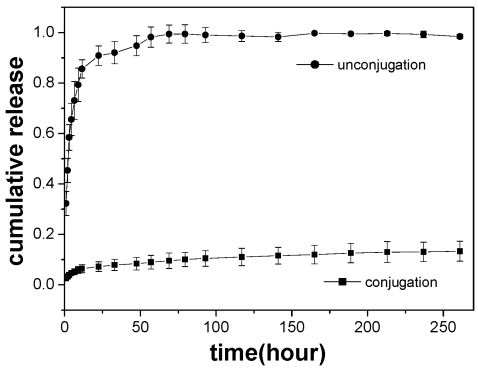

Fig. 7 Release profiles of DOX from DOX–Fe_3O_4–SiO_2 nanoparticles and silica nanoparticles containing physically-entrapped DOX.

Conclusions

A new one-pot procedure was successfully developed for the fabrication of drug conjugated magnetic silica nanoparticles using the widely used anticancer agent DOX as a model drug *via* a urea bond (–NHCONH–) through the reaction of the amino groups of DOX with the isocyanate group of ICPTES, followed by sol–gel polymerization of triethoxysilane. The obtained nanoparticles with mean diameter of 66.9 nm showed a good response to a magnetic field. The encapsulation efficiency of the DOX–SiO_2–Fe_3O_4 nanoparticles was evaluated to be 60.5 ± 3.7%. This is much higher than that of the control silica nanoparticles (7.3 ± 1.6%). The DOX–Fe_3O_4–SiO_2 nanoparticles showed a significantly lower drug release rate than the control silica nanoparticles due to the urea linkage (–NHCONH–) between the DOX and the inorganic nanoparticles. Therefore, the DOX–Fe_3O_4–SiO_2 nanoparticles have a great application potential in the treatment of cancer using magnetic targeting drug-delivery technology. The targeting of drug delivery under an applied magnetic field and possible accelerated release in the cancer cell is currently under study. The technique should be widely applicable for drugs containing –NH_2 groups. It is anticipated that fine-tuning of the other drugs or bioactive molecules to Fe_3O_4/SiO_2 nanoparticles will lead to the construction of a wide range of supramolecular architectures, fostering innovative avenues for the development of smart drug delivery and controlled release systems.

Acknowledgements

This research is financially supported by the National High Technology Research and Development Program of China (No. 2007AA03Z316), the Cultivation Fund of the Key Scientific and Technical Innovation Project, Ministry of Education of China (No. 707021), NSFC-20977021, National Natural Science Foundation of Heilongjiang Province (E-2007-12) and State Key Laboratory of Urban Water Resources and Environment (2008QN06).

References

1 L. Yu, Y. Gao, X. Yue, S. Liu and Z. Dai, *Langmuir*, 2008, **24**, 13723–13729.
2 J. Zheng, X. Yue, Z. Dai, Y. Wang, S. Liu and X. Yan, *Acta Biomater.*, 2009, **5**, 1499–1507.
3 S. Sengupta, D. Eavarone, I. Capila, G. Zhao, N. Watson, T. Kiziltepe and R. Sasisekharan, *Nature*, 2005, **436**, 568–572.
4 V. P. Torchilin, *Nat. Rev. Drug Discovery*, 2005, **4**, 145–160.
5 Z. Liu, C. Davis, W. B. Cai, L. He, X. Y. Chen and H. J. Dai, *Proc. Natl. Acad. Sci. U. S. A.*, 2008, **105**, 1410–1415.
6 J. H. Lee, Y. M. Huh, Y. Jun, J. Seo, J. Jang, H. T. Song, S. Kim, E. J. Cho, H. G. Yoon, J. S. Suh and J. Cheon, *Nat. Med.*, 2007, **13**, 95–99.
7 X. H. Gao, Y. Y. Cui, R. M. Levenson, L. W. K. Chung and S. M. Nie, *Nat. Biotechnol.*, 2004, **22**, 969–976.
8 S. Godefroo, M. Hayne, M. Jivanescu, A. Stesmans, M. Zacharias, O. I. Lebedev, G. Van Tendeloo and V. V. Moshchalkov, *Nat. Nanotechnol.*, 2008, **3**, 174–178.
9 M. Ferrari, *Nat. Rev.*, 2005, **5**, 161–171.
10 S. D. Caruthers, S. A. Wickline and G. M. Lanza, *Curr. Opin. Biotechnol.*, 2007, **18**, 26–30.
11 V. P. Torchilin, *Adv. Drug Delivery Rev.*, 2006, **58**, 1532–1555.
12 J. M. Kinsella and A. Ivanisevic, *J. Am. Chem. Soc.*, 2005, **127**, 3276–3277.
13 J. M. Perez, T. O'Loughin, F. J. Simeone, R. Weissleder and L. Josephson, *J. Am. Chem. Soc.*, 2002, **124**, 2856–2857.
14 J. M. Perez, F. J. Simeone, Y. Saeki, L. Josephson and R. Weissleder, *J. Am. Chem. Soc.*, 2003, **125**, 10192–10193.
15 L. E. Udrea, N. J. Strachan, V. Badescu and O. Rotariu, *Phys. Med. Biol.*, 2006, **51**, 4869–4881.
16 J. H. Park, L. Gu, G. von Maltzahn, E. Ruoslahti, S. N. Bhatia and M. J. Sailor, *Nat. Mater.*, 2009, **8**, 331–336.
17 C. Barbé, J. Bartlett, L. G. Kong, K. Finnie, H. Q. Lin, M. Larkin, S. Calleja, A. Bush and G. Calleja, *Adv. Mater.*, 2004, **16**, 1959–1966.
18 H. S. Yoo, E. A. Lee and T. G. Park, *J. Controlled Release*, 2002, **82**, 17–27.
19 H. S. Yoo and T. G. Park, *J. Controlled Release*, 2001, **70**, 63–70.
20 H. S. Yoo, K. H. Lee, J. E. Oh and T. G. Park, *J. Controlled Release*, 2000, **68**, 419–431.
21 M. R. Dreher, D. Raucher, N. Balu, O. M. Colvin, S. M. Ludemanc and A. Chilkoti, *J. Controlled Release*, 2003, **91**, 31–43.
22 K. Ulbrich, T. Etrych and P. Chytila, *J. Controlled Release*, 2003, **87**, 33–47.
23 Y. Bae, T. A. Diezi, A. Zhao and G. S. Kwon, *J. Controlled Release*, 2007, **122**, 324–330.
24 P. Chytil, T. Etrych, T. Mrkvan and K. Ulbrich, *J. Controlled Release*, 2008, **127**, 121–130.
25 P. Chytil and K. Ulbrich, *J. Controlled Release*, 2006, **115**, 26–36.
26 T. Etrych, M. Jelinkova, B. Rihova and K. Ulbrich, *J. Controlled Release*, 2001, **73**, 89–102.
27 A. Kakinoki, Y. Kaneo, Y. Ikeda, T. Tanaka and K. Fujita, *Biol. Pharm. Bull.*, 2008, **31**, 103–110.
28 F. Kratz, I. A. Muller, C. Ryppa and A. Warnecke, *ChemMedChem*, 2008, **3**, 20–53.
29 J. Khandare and T. Minko, *Prog. Polym. Sci.*, 2006, **31**, 359–397.
30 T. Ouchi and Y. Ohya, *Prog. Polym. Sci.*, 1995, **20**, 211–257.
31 F. H. Chen, Q. Gao and J. Z. Ni, *Nanotechnology*, 2008, **19**, 165103–165111.
32 A. M. Jordan, T. H. Khan, H. Malkin and H. M. I. Osborn, *Bioorg. Med. Chem.*, 2002, **10**, 2625–2633.
33 Y. Sahoo, A. Goodarzi, M. T. Swihart, T. Y. Ohulchanskyy, N. Kaur, E. P. Furlani and P. N. Prasad, *J. Phys. Chem. B*, 2005, **109**, 3879–3885.
34 T. T. Goodman, P. L. Olive and S. H. Pun, *Nanomedicine*, 2007, **2**, 265–274.
35 C. C. Berry and A. S. G. Curtis, *J. Phys. D: Appl. Phys.*, 2003, **36**, R198–R206.
36 P. Velazquez-Morales, J. F. Le Nest and A. Gandini, *Electrochim. Acta*, 1998, **43**, 1275–1279.
37 S. K. Park, K. Do Kim and H. T. Kim, *Colloids Surf., A*, 2002, **197**, 7–17.
38 B. J. Tan, K. J. Klabunde and P. M. A. Sherwood, *Chem. Mater.*, 1990, **2**, 186–191.
39 J. J. Moreau, L. Vellutini, M. W. Chi Man, C. Bied, J. L. Bantignies, P. Dieudonne and J. L. Sauvajol, *J. Am. Chem. Soc.*, 2001, **123**, 7957–7958.

